반도체및디스플레이장비학회지 제3권 제1호(2004년 3월)
Journal of the Semiconductor & Display Equipment Technology, Vol. 3, No. 1. March 2004.

Effect of Alternating Magnetic Field on Ion Activation in Low Temperature Polycrystalline Silicon Technology

Jin Ha Hwang[†]* and Tae Hyung Lim*

[†]*Dept. of Mat. Sci. & Eng., College of Engineering, Hongik University

ABSTRACT

Statistical design of experiments was successfully employed to investigate the effect of alternating magnetic field on activation of polycrystalline Si (p-Si) doped as n-type using PH_3, by full factorial design of three factors with two levels. In this design, the input variables are graphite size, alternating current, and activation time. The output parameter, sheet resistance, is analyzed in terms of the primary effects and multi-factor interactions. Notably, the three-factor interaction is calculated to be a dominant interaction. The interaction between graphite size and activation time and the main effect of current are important effects compared to the other variables and relevant interactions. Alternating magnetic flux activation is proved a significantly beneficial processing technique.

Key Words : Ion-doping, Activation, Sheet resistance, p-Si, DOE, Statistical analysis, Alternating current, Magnetic flux

1. Introduction

Liquid crystal displays (LCDs) possess the dominant position in flat panel technology currently. The LCDs have been combined with amorphous silicon (α-Si) thin film transistors (TFT). Recently, there has been significant evolution in display: low temperature polycrystalline silicon (LTPS) technology and organic electroluminescent materials [1]. LTPS transistors offer much higher mobilities ranging from 10-500 $cm^2/Vsec$, than those of the α-Si TFT ranging from 0.3-1.0 $cm^2/Vsec$ [2-4]. Higher mobilities reduce the size of the TFT leading to higher aperture ratio, reduce materials costs by incorporating the integration of driver ICs, and reduce the display module weight and thickness. In addition, it has higher potential of a complete system on glass, including the panel ASIC, memory, photodiodes, sensors, sound chips, etc. The second organic electroluminescent materials offer higher brightness, better color characteristics, and less weight in conjunction with LTPS transistors.

However, the realization of the commercial display-products faces challenges toward mass production with high yield, requiring strict inspection and testing with a nondestructive testing tool. Among essential processes in LTPS technology, are gate dielectric deposition, crystallization of α-Si into p-Si, and ion-doping. In particular, LTPS technology has been advanced, based on various crystallization techniques: e.g., solid phase crystallization, excimer laser annealing, rapid thermal annealing, metal-induced crystallization, etc [5-12].

The ion-doping process incorporates the activation of ions implanted into p-Si as p-type or n-type. Depending on type of ion-doping, condition of activation and dose amount, the resultant characteristics vary significantly in transistor performance. Ion-doping is performed in either mass-separation or non-mass separation in conjunction with implanter or shower type. The detailed activation processes are furnace-annealing, rapid thermal annealing, and excimer laser annealing [13, 14]. Recently, another activation process is introduced, i.e., alternating magnetic field annealing (AMFA) through induction system. Unlike the lengthy process time of thermal activation, e.g., 12 to 24 hours at 500 to 600°C, AMFA allows the rapid annealing time in ion-doped Si, leading to improvement in tact time of product manufacturing.

[†]E-mail : jhwang@wow.hongik.ac.kr

The current report will address the performance based on process variables using statistical approach, i.e., design of experiments. For effective transistors, the source and drain electrodes must have low sheet resistance which requires higher degree of activation. Therefore, sheet resistance is chosen as an output parameter. The current work reports the application of an statistical approach based on design of experiments and the applicability of alternative magnetic flux annealing as ion activation.

2. Experimental

The activation process was performed using an alternating field system as shown in Fig. 1. The frequency is 13.56 kHz. The alternating current ranges up to 50A. The alternating current is applied through induction coils. The alternating current changes the direction of magnetic fields as a function of the initial ac electric field. Initially, the preliminary vacuum is kept below 10^{-3} torr and purged using Ar atmosphere. Activation using AMFA is performed as a function of graphite size, current, and annealing time.

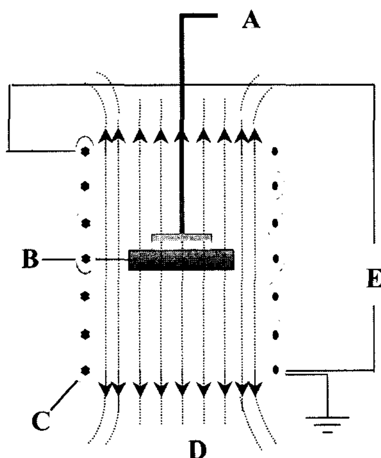

Fig. 1. Schematic aiagram of an alternating activation system. A: thermocouple, B: graphite susceptor, C: induction coil, D: alternating magnetic field, and E: ac electric field (frequency (13.56 kHz).

The full factorial design, 2^3 design created 8 different runs of the high and low values (denoted by +1 and 1 in coded values, respectively) in experimental variables, as shown in Table 1. The experimental variables are graphite, alternating current, and annealing time. The standard order was randomized to yield the actual run order in order to eliminate the time-dependent influence that is not a controllable factor. The detailed experimental conditions are depicted in Table 1 with the uncoded and coded values, along with the output values and the corresponding temperatures when the activation occurs.

Table 1. Experimental conditions for eight runs and calculated data. (A: graphite size [mmXmm], B: current [A], C: time [min.], Rs: sheet resistance [ohm/□], and Temp: temperature)[°C].

	A	B	C	Rs	Temp
1	40(−1)	45(−1)	20(+1)	659	630
2	40(−1)	50(+1)	5(−1)	694	700
3	40(−1)	50(+1)	20(+1)	776	700
4	45(+1)	45(−1)	20(+1)	925	712
5	45(+1)	45(−1)	5(−1)	651	712
6	45(+1)	50(+1)	5(−1)	566	800
7	40(−1)	45(−1)	5(−1)	1300	630
8	45(+1)	50(+1)	20(−1)	633	800

Amorphous Si is deposited on the SiO_2 (3000A)/glass (Corning 1737) at the thickness of 500A by plasma-enhanced chemical vapor deposition (PECVD). Subsequently the amorphous Si thin film is crystallized into polycrystalline Si through excimer laser annealing (wavelength of 308 nm with XeCl source). Ion-doping is conducted as n-type on the polycrystalline Si supported by glass substrate through ion shower doping of PH_3, doped through a non-mass separation technique. The specimens are cut into 10mmX10mm plates for activation test and electrical characterization. The electrical properties are measured using Hall measurement through a Van der Pauw configuration. The ohmic contact between electrodes and doped regions was confirmed, using a dc (direct current) four-point resistivity measurement technique on the identical specimens which exclude the nonohmic contributions at the electrode/semiconductor interface. In Hall measurements, the four microtips are placed on the corners of the squared specimens. Sheet resistance is calculated by taking into account geometric factors. Hall measurements confirmed the type of charge carriers.

3. Results and Discussion

Design of experiments allows estimation of importance of primary effects and interactions and modeling of the process under study, i.e., activation in ion-doping. The system can be modeled as the following

$$Y= \beta_0+\beta_1x_1+\beta_2x_2+\beta_3x_3+\beta_{12}x_1x_2+\beta_{13}x_1x_3+\beta_{23}x_2x_3+\beta_{123}x_1x_2x_3+\varepsilon \quad \text{Eq. (1)}$$

where x_1 represents factor A, x_2 represents factor B, x_1x_2 represents the two-factor interaction, specifically the AB interaction, and x_1 x_2 x_3 represents the ABC interaction. β_0 is the grand average of the observations, and β_1, β_2, β_{12}, β_{123}, etc are estimated by one-half of the corresponding effect values and ε is a random error [15]. Fortunately, the current work was performed through full-factorial design; three factors with two levels, leading to total of 8 experiments. The statistical results are summarized in Table 2 with regard to the output parameter, i.e., estimated effects and coefficients for sheet resistance. Figs. 2 and 3 represent the normal plot and Pareto chart of the estimated effects constructed according to Table 2. At the level of α=0.1, any factors are not statistically significant. The current work is analyzed in terms of applicability of the statistical approach, only considering the absolute magnitude of estimated effects. Since the current design does not employ fractional factorial design, all main effects and all interactions can be clarified. This will help understanding the main effects and the interactions without ambiguity. Typically, three-factor and higher-order factor interactions are assumed to be negligible in estimating the effects, leading to reduction of experimental effort. The assumption is not applied to the current case. However, the statistical significance should be judged on the level of α=0.1.

Table 2. Estimated effects and coefficients for sheet resistance

Term	Effect	Coefficient
Constant		775.5
Size	−163.5	−81.7
Current	−216.5	−108.2
Time	−54.5	−27.3
Size×Current	28	14
Size×Time	225	112.5
Current×Time	129	64.5
Size×Current×Time	−232.5	−116.3

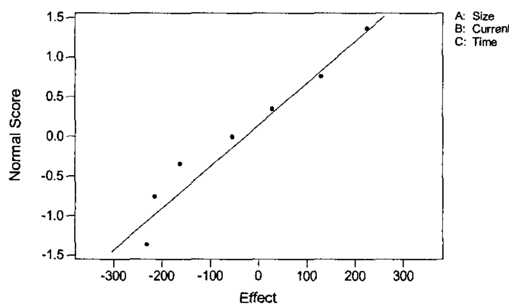

Fig. 2. Normal plot of sheet resistance at the level of α=0.1.

From Table 2, the main effects, i.e., the effects of graphite size, current, and annealing time are negative: i) the sheet resistance decreases with increasing graphite size, ii) the sheet resistance decreases with increasing the current, and iii) the sheet resistance decreases with increasing time. Among the three main effects, current is a dominant one. As shown in Fig. 4, the main effects of graphite size and current are larger than that of activation time. Activation time does not affect sheet resistance but the other two do.

From the interaction plot of Fig. 5, no interaction is

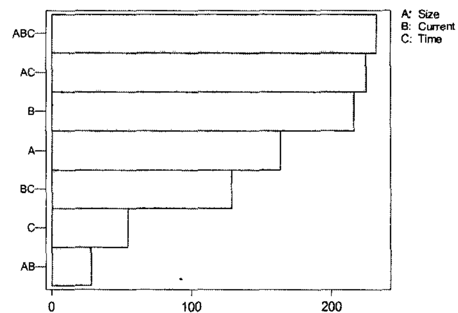

Fig. 3. Pareto chart of sheet resistance from activation experiment.

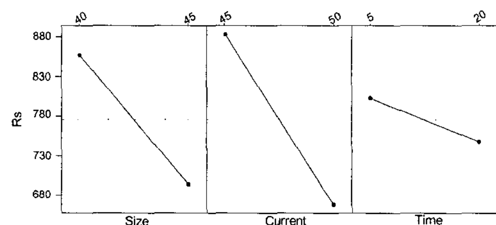

Fig. 4. Main effects plot from activation experiments.

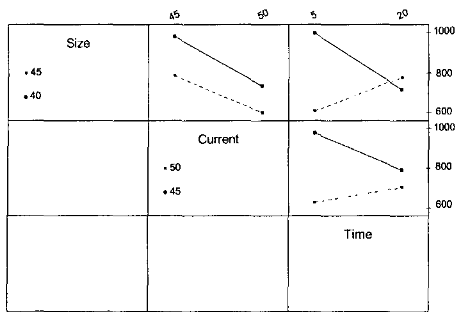

Fig. 5. Interaction plots from activation experiments.

found between graphite size and current, since the variation of current from low level to high level, induces approximately the same change in sheet resistance at both levels of graphite sizes, (−1: 40×40mm, +1: 45×45 mm). Contrary to that of graphite size, the interactions between graphite size and the activation time, and between current and activation time are not negligible. Relatively, the interaction between graphite size and activation time is higher than the other.

Notably the three-factor interaction is dominant in Pareto charts in magnitude with the negative sign. This result is in reasonable agreement with the signs of main effects which are negative respectively.

Activation through continuous wave laser exhibited two times higher than the conductivity obtained using thermal annealing [13]. Thermal annealing using furnaces are usually applied for 12 to 24 hours. Although rapid thermal annealing was employed at 1000°C in nitrogen[14], the current alternating magnetic flux annealing is performed for 5 minutes at 800°C. The current approach is proved to be more effective in terms of time and thermal budget toward mass production in the flat-panel displays.

Design of experiments using a factorial design is more efficient than an approach to change factors one at a time, in understanding the interactions between variables.

Above 700°C, longer activation leads to higher sheet resistance, indicating that deactivation takes place, through defect-dopant interactions, presumably. The relevant issue will be discussed in the following publications.

4. Conclusions

A 2^3 full factorial design was employed in order to estimate the effect of main effects and interactions in terms of graphite size, current, and time. The three-factor interaction, the interaction between graphite size and time, and current are listed as major interactions and effects in determining the sheet resistance, in the descending order. From the economic aspect in activation (time and temperature), the alternating magnetic flux annealing can be employed in activating the ion-doped glass substrates in the flat-panel displays incorporating low temperature polycrystalline Si technology. Furthermore, above 700°C, the deactivation occurs leading to higher resistance.

Acknowledgements

This research was supported by the 2002 Hongik University Academic Research Support Fund.

References

1. Komiya, N., Nishikawa, R., Okuyama, M., Yamada, T., Saito, Y., Oima, S., Yoneda, K., Kanno, H., Takahashi, H., Rajeswaran, G., Itoh, M., Boroson, M., and Hatear, T.K., "Active Matrix OLED Displays with Low-Temperature Poly-Si TFT," Proceeding of the 10th International Workshop on Inorganic and Organic Electroluminescence, pp. 347-352 (2000).
2. Sera, K., Okumura, F., Uchida, H., Itoh, S., Karelso, S., and Hotta, K., "High-Performance TFT's Fabricated by XeCl Excimer Laser Annealing of Hydrogenated Amorphous-Silicon Films," *IEEE Trans. ELectron Devices* Vol. 36, No. 12, pp. 2868-2871 (1999).
3. Crowder, M.A., Garey, P.G., Smith, P.M., Sposili, R.S., Cho, H.S., and Im, J.S. "Low-Temperature Single Crystal Si TFT's Fabricated on Si Films Processed via Sequential Lateral Solidification," *IEEE Electron Device Lett.* Vol. 19, No. 8, pp. 306-308 (1998).
4. Yamamoto, M., Nishitani, H., Sakai, M., Gotoh, M., Taketomi, Y., Tsutsu, T., and Nishitani, M., High Performance Low Temperature Poly-Si TFT Obtained by a New Fabrication Method," *Euro Display, 99 Proceedings,* pp. 53-56 (1999).
5. Ibok, E., and Garg, S.J., "A Characterization of the Effect of Deposition Temperature on Polysilicon Properties," *Electrochem. Soc.,* Vol. 140, pp. 2927-2937 (1993).
6. Lee, S.W., and Joo, S.K., "Low Temperature Poly Si

Thin Film Transistor Fabrication by Metal-Induced Lateral Crystallization," *IEEE Electron Device Lett.*, Vol. 17, pp. 160-162 (1996).

7. Lee, S.Y., Jeon, Y.C., and Joo, S.K. "Pd Induced Lateral Crystallization of Amorphous Si Thin Films," Appl. Phys. Lett., Vol. 66, No. 13, pp. 1671-1673 (1995).
8. Im, J.S., and Sposili, R.S., "Crystalline Si Films for Integrated Active-Matrix Liquid Crystal Displays," Mat. Res. Bull., Vol. 2, No. 3, pp. 39-48 (1996).
9. Lee, J.-B., Lee, C.-J., and Choi, D.-K., "Influence of Various Elements on Field-Aided Lateral Crystallization of a-Si Film," *Jpn. J. Appl. Phys.*, Vol. 40, pp. 6177-6181 (2001).
10. Song, A.R., A Study on The Solid Phase Crystallization of LPCVD a-Si Thin Films by Alternating Magnetic Flux. M.S. Thesis, Hongik University (2000).
11. Kakkad, R., Smith, J., Lau, W.S., Fonash, S.J., and Kerns, R., "Crystallized Si Films by Low-Temperature Rapid Thermal Annealing of Amorphous Silicon," *J. Appl. Phys.*, Vol. 65 pp. 2069-2072 (1989).
12. Park, K.-C., Song, I.-H., Jung, S.-H., Park, J.-W., and Han, M.-K., "The Composite Effects of MILC and ELA on the Crystallization of a-Si Film," AM-LCD 2000, pp. 147-150 (2000).
13. Gat, A., Gerzberg, L., Gibbons, J.F., Magee, T.J., Peng, J., and Hong, J.D., "CW Laser Anneal f Polycrystalline Silicon: Crystalline Structure, Electrical Properties," *Appl. Phys. Lett.*, Vol. 33, No. 9, pp. 775-778 (1978).
14. Kawasaki, Y., Murakami, T., Kuroi, T., Ohno, Y., and Matsui, Y., "Application of Non-Mass Analyzed Ion Implanter to Sub-quarter Micron MOSFETS," Mat. Chem. and Phys., Vol. 54, pp. 17-22, 1998.
15. Montgomery, D.C., and Runger, G.C., Applied Statistics and Probability for Engineers, pp. 505-570, John Wiley & Sons, Inc., 2002.